Canadian Science Publishing | Canadian Geotechnical Journal

Quantitative Risk Assessment of Rock Slope Instabilities That Threaten a Highway Near Canmore, AB, Canada: Managing Risk Calculation Uncertainty in Practice

Journal:	*Canadian Geotechnical Journal*
Manuscript ID	cgj-2018-0739.R2
Manuscript Type:	Article
Date Submitted by the Author:	24-Feb-2019
Complete List of Authors:	Macciotta, Renato; University of Alberta, School of Engineering Safety and Risk Management Gräpel, Chris; Klohn Crippen Berger Keegan, Tim; Klohn Crippen Berger Duxbury, Jason; Klohn Crippen Berger Skirrow, Roger; Government of Canada, Alberta Transportation
Keyword:	Quantitative Risk Assessment, Uncertainty, Risk Criteria, Rock Fall, Decision-making
Is the invited manuscript for consideration in a Special Issue? :	Not applicable (regular submission)

Quantitative Risk Assessment of Rock Slope Instabilities That Threaten a Highway Near Canmore, AB, Canada: Managing Risk Calculation Uncertainty in Practice

Renato Macciotta (Corresponding Author)
School of Engineering Safety and Risk Management, University of Alberta
12-324 Donadeo Innovation Centre for Engineering, Edmonton, AB T6G 1H9
Email: macciott@ualberta.ca
Phone: +1 (780) 862-4846

Chris Gräpel
Klohn Crippen Berger
301, 2627 Ellwood Dr SW, Edmonton, AB T6X 0P7
Email: cgrapel@klohn.com

Tim Keegan
Klohn Crippen Berger
301, 2627 Ellwood Dr SW, Edmonton, AB T6X 0P7
Email: tkeegan@klohn.com

Jason Duxbury
Klohn Crippen Berger
301, 2627 Ellwood Dr SW, Edmonton, AB T6X 0P7
Email: jduxbury@klohn.com

Roger Skirrow
Alberta Transportation
2nd Floor, 4999-98th Avenue, Edmonton, AB T6B 2X3
Email: Roger.Skirrow@gov.ab.ca

Abstract:

We present a quantitative risk assessment (QRA) to guide decision-making for selection of rock fall protection strategies. The analysis corresponds to a section of highway near Canmore, Alberta, Canada; where rock falls are common. Environmental concerns, tourism and economic activities overlap the project area and increased the complexity of the decision-making process. QRA was adopted to improve highway user safety and minimize effects on natural, social and economic environments. Uncertainty was associated with hazard and consequence quantification, and the study elicited plausible ranges of input variables for risk calculation. Expected and range in risk were calculated for current conditions and after mitigation. Individual risk to highway users was found to be low, following the limited exposure of any particular individual. Current total risk was calculated at 2.9 x 10^{-4} probability of fatality and a plausible range between 2.0 x 10^{-5} and 5.5 x 10^{-3}. The slope protection configuration selected had a residual total risk between 9.0 x 10^{-4} and 2.9 x 10^{-6}, and a best estimate of 4.5 x 10^{-5}. The risk levels were evaluated against criteria previously used in Canada and were considered a appropriate balance between project costs, public safety, environmental concerns, tourism, and economic activities after mitigation.

Key Words:

Quantitative Risk Assessment, Uncertainty, Risk Criteria, Rock Fall, Decision-making

Introduction

The adoption of quantitative risk assessments (QRA) for landslide management decision-making has increased over the last few decades (Morgenstern 1997; ERM 1998; Kong 2002; Mostyn and Sullivan 2002; El-Ramly et al. 2003; Bonnard et al. 2004; Fell et al. 2005; Lacasse et al. 2008; Cassidy et al. 2008; Lu et al. 2014; Corominas et al. 2014; Vranken et al. 2015; Uzielli et al. 2015; Macciotta et al. 2016). Particularly in Western Canada, quantified risk has become the basis for decision-making regarding development upon landslide-prone areas (VanDine 2018). Examples include the District of North Vancouver (Hungr et al. 2016) and the proposed Cheekeye Fan Development (Clague et al. 2015) in the province of British Columbia, and the debris flow/flood protection works for Canmore, in the province of Alberta (Hungr et al. 2016).

However, landslide QRA is associated with a number of challenges (Ho et al. 2000; Crozier and Glade 2005). These include: 1) the required input of judgment to elicit the probabilities needed to populate the analysis of landslide occurrence and/or its consequences, and 2) the adoption of risk evaluation criteria. The first challenge is associated with increased uncertainty in the calculated risk. Ways forward include: adopting consequential risk assessments; relative decrease in risk after mitigation, and; the use of calculated ranges of risk values. The second challenge is associated with social, political and economic implications and associated expectations, policies and consequences. Ways forward include robust risk understanding, communication and public consultation, and adoption of a country-wide set of criteria.

This paper presents the risk-based decision-making process used to select the mitigation strategies along a section of highway threatened by rock falls. The site is regarded for its significance to wildlife (as a wildlife movement corridor), recreational activities (as a rock climbing area), scenic tourism corridor and is adjacent to a reservoir perched high above Canmore. QRA was adopted to better balance the safety of highway users with minimizing the impacts to the environment and recreational activities. Decision-making followed a QRA for the existing conditions and for different mitigation options, evaluated against risk criteria used in Canada. This paper focuses on the QRA for the site and detail discussion on the social and environmental aspects is out of the scope of the paper. QRA was the tool used to evaluate that risks were within tolerable thresholds for the mitigation options proposed, after any modifications that would follow social and environmental considerations. The landslide risk assessment process followed the outline and recommendations in Fell et al. (2005) and Corominas et al. (2014). This process defines the scope of the assessment, calculates failure volumes and their likelihood as a measure of hazard. The process then calculates landslide run out, velocities, impact energies, impact likelihoods, and vulnerability as a measure of consequences. Hazard and consequences combine to provide the levels of risk that are evaluated against the selected criteria. The following sections present the characteristics of the study area, the calculations and required judgment to elicit the probabilities to establish the hazard, consequence and risk values. In addition, an evaluation of the current conditions and proposed mitigation against risk criteria previously used in Canada is provided. This paper highlights the uncertainty associated with risk estimations and the approach adopted to

address these uncertainties and mitigate their impact in the decision-making process for managing risks.

The S042 Rock Slope

Location

The S042 site is located on Alberta Highway 742 (also known as Spray Lake Trail), at the entrance to the Spray Lakes valley approximately 5 km southwest of Canmore, AB (Figure 1). Figure 2a presents a plan view of the rock slope showing slope Sectors A through F for reference through this paper, and rock debris window mapping Locations 1 through 7. Figure 2b shows a representative photograph of the rock slopes. This figure shows the loose talus slope that extends from the edge of the gravel highway (there is no ditch) at approximately 40 degrees and to a near vertical rock cliff face approximately 80m high. Alberta Transportation (AT) manages this section of Highway 742, identifying this rock slope as the S042 site in their Geohazard Risk Management Program.

Geologic Context and Climate

The S042 site is at the southeast end of the Mount Rundle range which is a part of the South Banff Ranges oriented southeast-northwest. Its steep, rocky and bare nature contrasts with the gentle and forested physiography of the Bow valley to the east. There are seven distinct summits along the Mount Rundle range, the highest is at an elevation of 2,948 m. The highway through Whitman's Pass, immediately beneath East Rundle is at elevation 1715m, while the

adjoining Bow valley is between elevation 1,300 m and 1,400 m. Mount Rundle consists of Paleozoic limestones, dolomitic limestones, dolostones and shales thrusted onto Mesozoic sedimentary rocks outcropping in the Bow valley. Bedding planes dip at 41° towards the southwest (Price 1970). The S042 rock slope has a general orientation in the southeast direction, with slope sections dipping within a range between east and south.

Based on data collected between 1981 and 2010 at a station 29 km to the southeast, the average daily temperature ranges between -6.1°C in January and 14.5°C in July (Environment Canada 2016). The average daily maximum temperature ranges between -1.0°C and 22.1°C, while the minimum ranges between -11.7°C and 6.8°C. Extreme temperatures can reach 34.5°C and –45.6°C during the Summer and Winter, respectively. Monthly precipitation ranges between about 19 mm in December and 119 mm in June, for a total annual precipitation of 647 mm per year. Between October and April, most precipitation consists of snow.

Previously Proposed Mitigation

Work in the area consists of site investigations, detailed structural mapping, ground and air photogrammetry, and rockfall trajectory modeling (KCB 2016). These studies led to proposed mitigation options that included the use of catch fences at the toe of the talus slope (6 m to 9 m in height and 800 KJ impact energy), ditch widening, upslope catch fences / attenuator systems, visual inspections for loose blocks, long-term monitoring and establishment of trigger response protocols for potential large instabilities (KCB 2016). The catch fence / attenuator system consists of a high strength steel wire mesh curtain hanging at certain elevation from the rock face and with the capacity to capture falling blocks from higher elevations and attenuate their

energies as the blocks are diverted towards the toe of the slope by the hanging mesh. These systems were required at a 70 m-long section mid-slope north of Sector D and Sector C in Figure 1 and a 70 m-long section in Sectors D and E. AT's option selection corresponded to technical feasibility and efficiency in hazard reduction. A sketch of the location of these systems in shown in Figure 3.

Consultation with Alberta Environment and Parks (AEP) was done through a joined field assessment. AEP observations and information exchange in the field highlighted that the S042 site is a primary wildlife passage corridor through the valley and that it would be detrimentally affected by the proposed mitigation. Moreover, the proximity of this site to the active town of Canmore and the scenery of the area have led to a variety of activities, including wildlife photography, hiking, and rock climbing. These considerations added a layer of complexity regarding potential engineered structures for rock slope safety. In this regard, adoption of mitigation strategies to reduce risks to highway users required minimizing the potential impacts to wildlife and recreational activities. A risk-based decision-making approach was adopted to this end.

Rock Slope Hazard Analysis

Site Investigations and Observations

Site Investigations

Investigations focused on identifying potential failures and estimating rock fall debris volume distributions. This was done through observations of the rock slope and debris window mapping at 7 locations (Figure 2). Manual and virtual structural mapping through terrestrial photogrammetric models were also undertaken. The average volume of blocks at the base of the talus slope was found to be 0.3 m^3, with a maximum volume of 3.8 m^3.

Large blocks were observed at the base of a 2013 rock fall event and adjacent to the highway (Figure 4b). However, large blocks generally do not reach the base of the talus slope. It was assessed that large blocks falling individually would fragment upon impact on the talus slope or would not bounce or roll due to their shape and weight. Consequently, these larger blocks would likely slide on the talus slope and stop uphill from the highway (Figure 4a). Based on this observation, it was judged that 0.3 m^3 is a representative volume for individual rock falls reaching the road.

Results of structural mapping are shown in Table 1. A crude estimate of potential rock fall volumes can be obtained by multiplying discontinuity spacing (Macciotta and Martin 2015). Spacing for J1, J2 and S0 renders a maximum volume of 2.7 m^3, and an average of 0.15 m^3, values smaller than those observed but consistent with their order of magnitude.

Kinematic analyses based on information in Table 1 indicated:

- Planar sliding is marginally possible on east facing rock slopes and possible along northeast facing rock slopes.
- Wedge failure is possible.
- Flexural toppling is marginally possible on northeast facing rock slopes but unlikely to happen because the required joint set is not ubiquitous and with close spacing.

None of the failure mechanisms highlighted above were observed at the S042 site in large volumes, likely because measured persistence is short (Table 1) and persistent discontinuities are relatively infrequent. This suggests that rock detachments require cohesion loss to make block movement kinematicaly feasible, following precipitation, temperature, seismic, wind, wildlife, or anthropogenic triggers.

Field Observations

Blocks at the toe of the talus slope varied from weathered, sub-angular blocks to fresh (no perceptible weathering) angular blocks. The angular blocks were considered to have detached from the rock face more recently than the weathered blocks, however a quantitative estimate for their time of detachment is indeterminate with the available data. Some angular, fresh blocks, equal and less than 0.3 m in equivalent diameter were found along the west side the highway at the toe of the talus slope and along the east side of the highway, adjacent to a traffic barrier, as shown on Figure 5. A subset of these blocks might have been encountered on the road and moved to the side by maintenance staff or highway users. Approximately 50 rock blocks with equivalent diameters between 0.3 m and 0.6 m were found to have been contained

by an existing 2 m high catch fence (downslope sectors D and E – Figure 4b). These blocks would have travelled downslope to the road surface if not for the catch fence at that location.

The potential for failure of large slope volumes (up to 1000 m^3) exists and would require interactions of complex failure mechanisms and triggers. Field observations evidenced the potential development of persistent failure surfaces along a combination of bedding planes, fractures, joint families, and other discontinuities; which could cause progressive failure of the intact rock (Figure 6). Field observations that suggest the potential for larger slope failures included differential weathering, increased rock mass disaggregation, and the presence of opened discontinuities.

Window mapping of debris

Window mapping of rock block volumes was performed in 7 locations along the toe of the talus slope (red points in Figure 2). This improved understanding the volume - frequency distribution of blocks reaching the highway, without considering the larger blocks observed at higher locations within the talus slope. The area and number of surveyed blocks is shown in Table 2. Figure 7 shows the histogram of surveyed block volumes. Table 2 confirms that most blocks that reach the highway are equal or smaller than 0.3 m^3.

Highway Maintenance Observations

AT's maintenance contractor provided qualitative observations that evidenced a peak on rock fall activity during the winter and spring months, including June; when most precipitation, freeze-thaw cycles and spring thaw occur. This is consistent with rock fall activity in other areas

in the Canadian Cordillera (Macciotta et al. 2017a). Maintenance crews reported one hour of material removal every day between February and June, mostly removed by a grader or by hand, suggesting a relatively steady but small volume of debris. The S042 site is part of a larger area from which the data reported is collected (no specific rockfall locations are recorded). A conservative assumption is that blocks reach the highway daily between February and June. Anecdotal observations of small rock falls heard during site inspections and small blocks observed near the road shortly after road clearance, support this assumption. According to maintenance crews few rock fall occurrences happen during other months.

Hazard Quantification

Failure Volume-Frequency Relationship

Information presented was used to estimate volume-frequency relationships of blocks reaching and potentially blocking the highway, as well as the potential for larger events. Failure volume - cumulative frequency plots are common for calculating failure frequencies (Hungr et al. 1999). Figure 8a presents the relative cumulative frequency of the surveyed blocks. The survey focused on blocks adjacent to the highway, therefore discriminates for larger blocks found embedded in the talus slope at higher elevations. This relationship can be scaled to the annual frequency of rock falls reaching the highway. From maintenance observations a conservative assumption is that rock blocks reach the highway toe daily between February and June, with few occurrences the rest of the year. This would equate to approximately 100 blocks equal or smaller than 0.3 m^3 each year reaching the highway at the S042 site. This was the anchor point to produce the cumulative frequency plot in Figure 8b.

Extrapolating the frequency-volume relationship in Figure 8b to volumes over 10 m^3 is very uncertain. Slope deformation processes and level of rock mass disaggregation need to be considered for eliciting the expected frequency of larger failures. These were produced based on the information presented and are summarized in Table 3. Frequencies for rock fall volume ranges are calculated from Figure 8 by subtracting the cumulative frequency of the upper volume boundary from the cumulative frequency of the lower volume boundary. These ranges were established based on their perceived hazard and were adjusted iteratively based on the outcomes of the consequence analysis. Table 3 includes the rationale behind the selected frequencies.

Rock Fall Simulations

Rock fall trajectory simulations in two dimensions (RocFall software from Rocscience Inc. 2013) were used to calculate run-out distances, heights and velocities of falling blocks. The software models free fall of blocks along parabolic trajectories, the block impact with the ground and subsequent rebound and rolling. Simulations were done for six representative sections (Figure 9a). Rock fall sources were selected randomly within the uppermost third of the slope, however sources were manually selected when overhanging blocks or a sharp topographic change were observed in the field or cross section. The rock fall simulation is initiated by selecting a vertical offset height from the slope's rock fall source and an initial horizontal velocity. Macciotta and Martin (2013) showed that for slope cuts adjacent to transportation corridors, the initial velocity had no major effect on rock fall trajectory heights and velocities when reaching the transport infrastructure. Rock fall simulations in this study initiated at different locations on

the rock face with an initial vertical offset height of 0.5m and a horizontal velocity of 0.1 m/s. The offset height and horizontal velocity aim to avoid localized topographic variations that could stop movement at the trigger area. The low horizontal velocity aims to model the initial velocities immediately after block detachment. Energy loses could not be calibrated due to the lack of reliable field evidence and typical values from calibrated for the Canadian Cordillera (Lan et al. 2007; Lan et al. 2010; Macciotta et al. 2011) were used (Table 4). Friction angles of 15° and 20° were used for hard rock surfaces and talus surfaces, respectively, to model rolling blocks.

A typical section (cross section 3 in Figure 9a) is shown in Figure 9b with the results of the trajectory model output for existing conditions. This figure clearly indicates the model-predicted potential for blocks to reach the road at various heights and velocities.

Consequence and Risk Estimation

Consequence Estimation

Consequence estimation is limited to potential loss of life of highway users given a slope failure occurs. This includes vehicles travelling on the highway and does not include other activities such as the presence of climbers or hikers. Limiting the analysis to highway users corresponds to the jurisdiction extents of the ministry of highways. Potential risks for these other activities were addressed qualitatively and recommendations transmitted to the corresponding organizations. Estimation considers two scenarios: falling debris impacts a moving vehicle, and

moving vehicle impacts a blocked track. At this location the highway is barely two lanes wide, bounded by a rigid barrier on the reservoir side and an ominous rock slope on the other site. The scenario where a vehicle remains stationary was not considered representative given the narrow section of highway and the presence of a nearby informal parking area.

Consequence is measured as likelihood for a fatal incident to occur given a rock slope failure. The processes leading to a fatal incident were modelled using an event tree analysis (Macciotta et al. 2016; Macciotta et al. 2017b) to estimate consequence likelihoods (Figure 10).

The probability for a fatal occurrence, given a rock slope failure of a particular failure volume group ($P[F]$, where *F* indicates fatality) is calculated as:

$$P[F] = (P[S] \times P[F - fb]) + (P[B] \times P[blocked] \times P[i] \times P[F - bh]) \quad (1)$$

Where $P[S]$ is the spatial (*S*) probability that falling debris impact a vehicle, $P[F - fb]$ is the probability of fatality [*F*] given falling debris impact a vehicle [*fb*], $P[B]$ is the probability that fallen debris block [*B*] the highway, $P[blocked]$ is the probability that a vehicle encounters the blocked section of highway before maintenance crews clear the area, $P[i]$ is the probability that the vehicle impacts [*i*] the debris given it encounters the blocked section of highway, $P[F - bh]$ is the probability of fatality [*F*] given a vehicle impact with the debris [*bh*].

The binomial theorem is used to calculate the annual probability of fatality, considering the expected frequency of rock slope failures for each failure volume group (Table 3) (Bunce et al. 1997; Macciotta et al. 2016; Macciotta et al. 2017b):

$$Probability\ of\ fatality\ (for\ a\ given\ volume\ group) = 1 - (1 - P[F])^N \quad (2)$$

Where N is the estimated frequency of rock slope failures according to Table 3. Overall probability of fatality for highway users, is then calculated by summation over the failure volume ranges; and is the metric used for calculating risk:

$$Risk = \sum_{j\,=\,smallest\ volume\ group}^{j\,=\,largest\ volume\ group} 1 - (1 - P[F_j])^{N_j} \quad (3)$$

The following subsections present the estimation and justification for populating the analysis.

Falling block/debris impact a moving vehicle - $P[S]$

$P[S]$ depends on vehicle size and speed. It is a combination of the spatial and temporal probability that vehicle and material coincide at the same highway mileage ($P[Sm]$) and the probability that the material impacts or reaches the same lane where the vehicle is travelling (right or left lane - $P[Sw]$):

$$P[S] = P[Sm] \times P[Sw] \quad (4)$$

$P[Sm]$ can be estimated as:

$$P[Sm] = \frac{L \times C}{V \times 24} \quad (5)$$

Where L (in km) is the longest of: vehicle length or width of debris as they fall; C is the average number of vehicles per day and V is the vehicle speed in km/h. The average daily traffic along this section is 1260 vehicles according to AT (personal communication) for 2015. Seasonal traffic variations are expected through the year. Visitors are common all year in this area, and the anticipated range of average daily traffic was set between 500 and 3000 vehicles.

The speed limit in the area is 50 km/h, with a recommended speed of 35km/h when approaching the rock face. Moreover, the highway has restricted sight lines and is a roughly graded gravel road at this section. If vehicles travel over the speed limit, which has been observed in the area, road conditions limit vehicle speeds to approximately 60 km/h. Vehicles would typically travel closer to the suggested speed (about 40 km/h) following the road signal and many in appreciation of the scenery, however speeds are mostly dictated by weather conditions. A conservative maximum speed of 70 km/h was adopted as plausible to consider potential dry summer road conditions, variations in visibility conditions, and observed over speeding. Average car length is estimated at 5 m. $P[Sm]$ calculations are presented in Table 5. In this table, absolute lower and upper bounds are calculated based on the range of values adopted for L, C and V. However, the number of vehicles and their speeds heavily depend on weather conditions, where good weather is correlated with increased number of vehicles and increased speeds. Moreover, it was observed that the estimated baseline traffic (C = 500) would correspond to regular commuters, which typically use personal smaller vehicles. In this regard, using absolute ranges for $P[Sm]$ would render results that are not a reflection of the real conditions. Table 5 shows the upper and lower bounds used for analysis, which consider the correlation between L, C and V.

$P[Sw]$ was elicited comparing the volume of fallen material and the average width of vehicles with respect to the width of the highway (two lanes). The highway width varies between 8 m and 12 m along the site (lanes plus auxiliary area and shoulder), and the average car width is taken as 1.5 m to 2 m. With this information and the results from rock fall simulations described, elicited values for $P[Sw]$ and their justification are presented in Table 6.

The probability of fatality given a vehicle gets impacted ($P[F-fb]$) depends on the impact location, the volume of material and its velocity. There are not enough case studies on rock falls impacting vehicles that allow statistical estimations of fatality probabilities in this scenario. The study required adopting a number of conservative and rational assumptions and the probability of fatality given a vehicle gets impacted, and its justification, is shown in Table 7.

Moving vehicle impacts block/debris on highway

The probability a vehicle impacts a block/debris blocking the highway consisted in 1) the probability that the highway gets blocked after failure ($P[B]$), multiplied times 2) the probability a vehicle encounters the blocked highway (maintenance crews do not reach it first) ($P[blocked]$), multiplied times 3) the probability the driver does not maneuver around the blocked section or stop, therefore impact occurs ($P[i]$). Calculations start with the probability that a rock fall event reaches the highway, therefore the material either impacts a vehicle or blocks the highway (conservatively neglects the low chance that the blocks will shoot towards the adjacent water body). $P[B]$ can then be estimated as the probability that the block does not impact a moving vehicle:

$$P[B] = 1 - (P[Sm] \times P[Sw]) \quad (6)$$

This assumes that if a vehicle is impacted, all other traffic would come to a stop. This assumption is uncertain and conservative approach is assuming the highway will be blocked also when impacting a moving vehicle. $P[B]$ is therefore adopted as 1.

$P[blocked]$ depends on the probability that the highway is not cleared from debris by maintenance crews before a vehicle reaches the section ($1 - P[cleared]$). $P[cleared]$

(probability the highway is cleared) is estimated as the ratio of number of daily inspections (planned or unplanned) to the number of vehicles. Crews travel the section 10 times on any given day (conservative assumption based on personal communication – Alberta Transportation) and considering the average daily traffic; this represents less than 0.01 chance the road would be cleared before another vehicle reaches the section. A conservative assumption was adopted that if a rockfall blocks the highway, a vehicle will find it before it is cleared off ($P[blocked]$ was adopted as 1).

$P[i]$ depends on the volume of material, driver reaction, driver's unobstructed view ahead of the road (sight distance) and stopping distances. Sight distance at the S042 site exceeds 100 m, with the exception of foggy conditions. The Government of Queensland (2017) provides stopping distances for different vehicle speeds (including driver reaction distance). These are shown in Table 8. These stopping distances are generic and they vary depending on vehicle factors (e.g. vehicle type, age, maintenance history), driver factors (e.g. reaction time, level of driving skills) and road factors (dry or wet conditions, presence of ice or snow, paved or gravel road). These stopping distances relative to sight distance were used as input for estimating the likelihoods of impacting fallen debris and the likely speeds at impact. There are longer sight distances along this section of highway compared to the generic stopping distances, which suggests that drivers should be able to stop or significantly reduce the vehicle speed. Adopted values of $P[i]$ and their justification are presented in Table 9.

The probability of fatality given a vehicle impacts a blocked section of highway ($P[F - bh]$) depends vehicle speed and volume of the fallen material. Richards (2010) presents the probability of fatality to car drivers when colliding at different speeds. Here, "Delta-v"

represents the change of speed during impact. His findings are shown in Figure 11. Table 10 presents the probability of fatality at the speeds considered representative along the S042 site, and half the speeds. Half speeds are shown to illustrate the rapid reduction in fatality probability as speeds are reduced. This is used to elicit fatality probabilities for analysis considering driver will maneuver and reduce the speed before impact (Table 11).

Risk Calculation and Uncertainty – Current Conditions

Risk Calculations followed the event tree in Figure 10. Vehicles travelling along the S042 site have one to four occupants such that fatal incidents are considered to involve 4 people or less. Total risk (probability of fatality – one or more) and individual risk criteria was used for evaluation. Calculations for the annual average risk to highway users at the S042 site (total risk) are shown in Figure 12. Total risk was calculated at 2.9×10^{-4} probability of fatality. This calculation considers the estimated failure frequencies and average daily traffic and speeds.

Daily traffic varies throughout the year leading to variations in vehicle exposure. Rock fall frequencies are also known to vary throughout the year. Ranges of risk would capture this variability better than one estimated value. Moreover, the necessary input of elicited probabilities required to quantify risk is associated with uncertainty in the evaluation. This can also be addressed calculating ranges of risk. Here, risk values associated with worse and most favourable, plausible scenarios were estimated as a proxy for understanding risk variability and uncertainty; therefor providing a more informed assessment. Risk calculations were performed considering: 1) 10-fold increase in failure frequencies coinciding with maximum expected traffic and speeds (highest risk scenario), and 2) decrease in failure frequencies to 1/10 and minimum

expected traffic and speeds (lowest risk scenario) (Figure 13). It was estimated a plausible total risk range between 2.0 x 10^{-5} and 5.5 x 10^{-3} (annual probability of fatality).

The risk values calculated thus far correspond to the probability of a fatal accident per year. However, the risk to any particular individual will depend on the exposure of this individual to the rock slope. In this study, individual risks were estimated based on the expected exposure of those individuals that more frequently travel this section of highway. It was estimated that regular commuters in the area would have the highest exposures, between 2 and 10 times daily driving along the S042 site (workers in the area and highway maintenance crews). This exposure (2 to 10 times daily) can be compared to the daily traffic estimates (minimum 500 and maximum of 3000 vehicles). As a result, the individuals most exposed to the rock slope have a reduced exposure somewhere between 0.7 x 10^{-3} (2 of 3000) and 0.02 (10 of 500) when compared to the total exposure (all individuals). Given this rough estimate (e.g. not accounting for holidays, sick days, increased travel due to errands, etc.), this study adopted a range of 1 x 10^{-2} and 1 x 10^{-3}. The individual risk calculated with these exposures therefore ranges between 2 and 3 orders of magnitude lower than the calculated total risk. Individual risk upper bound for the higher ranges is estimated at 5.5 x 10^{-5} with a best estimate between 2.9 x 10^{-7} and 2.9 x 10^{-6}.

Residual Risk Calculation and Uncertainty – Designed Mitigation

Risk mitigation options evaluated included rock fall catchment structures at the toe of the slope (flexible catch fences and containment ditch), regular scaling, attenuator and wire mesh curtains on the rock face, increased public awareness, and monitoring for potentially large

failures (over 100 m^3). Evaluation was based on risk reduction relative to existing conditions and focused on protection structures. The process was iterative, following the steps for risk quantification described and reducing the frequency of rock falls reaching the road. This section presents the risk calculation for the mitigation strategy selected as the best option for minimizing intervention on the slope and achieving tolerable safety.

Rock fall trajectory models suggested most blocks could be intercepted at the toe of the talus slope with a 6m-high catchment fence. It intercepts between 95% and 99% of falling trajectories, except at Sectors D and E, and a section north of Sector D (about 85%). An attenuator and hanging wire mesh curtain at Sectors D and E (rock outcrop closest to the highway) intercepts between 95% and 99% of trajectories.

Falling velocities modelled reached 30 to 40 m/s. However, observations suggest most blocks reach the highway rolling at slower velocities. A 3000 KJ catch fence would be capable of stopping all blocks with volumes equal or smaller than 1.3 m^3 at the higher velocities and 3 m^3 blocks at half the maximum model velocities (20 m/s). These would also provide enhanced protection against larger failure debris considering these will disaggregate into smaller blocks. Table 12 shows the elicited probability of catchment for a 3000 KJ fence at the toe of the talus slope with an attenuator and hanging wire mesh curtain at Sectors D and E.

Monitoring large potential instabilities is considered part of the mitigation option. The effect of monitoring will be to reduce exposure of highway users to these larger failure volumes (100 to 1000 m^3) by closing the road when displacements suggest impending failure. Monitoring therefore reduces $P[Sm]$ for the largest failure volume group. To account for uncertainties in monitoring interpretation and response, it was assumed a chance of one in a hundred that

interpretation and response will not be adequate. $P[Sm]$ is reduced by 99% for the largest volumes. Calculations of the residual total risk after implementation of the mitigation options are presented in Figure 14, with a maximum range of 9.0 x 10^{-4}, a minimum range of 2.9 x 10^{-6} and a best estimate of 4.5 x 10^{-5}.

Considering the 2 to 3 order of magnitude reduction for estimating individual risks, as previously discussed, the maximum range for the estimated individual risk is 9 x 10^{-6}, with a best estimate between 2.9 x 10^{-8} and 2.9 x 10^{-7}.

Risk Evaluation

Risk evaluation requires the adoption of risk criteria. The criteria developed for landslide risks in Hong Kong (GEO 1998) has been the basis for previously used criteria for landslide risk evaluation in Canada: District of North Vancouver (Hungr et al. 2016), the Cheekye river landslide risk assessment in British Columbia (Clague et al. 2015) and debris flow and flood risk assessments for Canmore (Hungr et al. 2016). These criteria were also suggested for this study. Total risk (probability of fatality – one or more individual) was evaluated against the tolerable and acceptable societal criteria by GEO (1998) (Figure 15a). Here, acceptable is understood as not requiring further reduction, above the tolerable threshold requires immediate action (stop activity or reduce risk) and the region As-Low-As-Reasonably-Practicable (ALARP region) requires reduction of risk within technical, environmental and economic feasibility. Individual risk criteria in GEO (1998) consider tolerable individual risk for existing conditions equal or less than 1 in 10 000 and for new developments equal or less than 1:100,000. Given the present

highway use, the individual risk criteria for existing conditions was proposed (Figure 15b). As a reference, the individual criteria proposed by the Health and Safety Executive in the U.K. (HSE 2001) is also shown. These criteria are widely used for several activities and industries and provide a useful benchmark. Mortality rates in Canada are also shown for benchmark.

Individual risks (and maximum ranges) are well below GEO's criteria (Figure 15b). These are also within HSE's tolerable thresholds for the public. This corresponds to the low daily exposure of particular individuals to the S042 site. This level of risk is below the Canadian mortality rates caused by accidents (Statistics Canada 2012).

The estimated total risk is within tolerable thresholds by GEO (Figure 15a), however the maximum estimated range is well above the tolerable threshold. This corresponds to uncertainty in calculations and potential risk fluctuation. The proposed criteria suggest that risks require mitigation. The criteria for selecting the mitigation option aimed to reduce the total risk such that maximum ranges are within GEO tolerable thresholds. In this way, risk tolerability is achieved minimizing the effects on wildlife and recreational and economic activities.

The residual risk ranges are plotted in Figure 16 and suggest total risks can be lowered within GEO tolerability criteria (Figure 16a) with implementation of the proposed mitigation. Best estimate for individual risk is further reduced within acceptable thresholds, with maximum values at the mid range of the ALARP zone (Figure 16b). These imply the mitigation proposed would meet the ALARP criterion.

The relative increase in safety after implementation of mitigation was calculated to provide further insight when evaluating the effectiveness of mitigation. Implementation would reduce risk approximately an order of magnitude, which was considered adequate for the proposed protection work.

Discussion and Conclusion

This paper presents a case study of quantitative risk assessment for decision-making regarding adoption of rock fall protection strategies. Rock falls that threaten highway users were estimated between 0.3 and 3.8 m^3, with some areas showing the potential for larger events. The site presented challenges associated with environmental concerns and economic activities (e.g. wildlife conservation, tourism) that increased the complexity of the decision-making process for rock slope mitigation strategies. A quantitative risk assessment was adopted to achieve the required balance between public safety and minimum impact on the environment and, social and economic activities. All the analysis focused on highway users along the highway and risk metrics were total annual risk of fatality (probability of fatality – one or more) and individual risk.

Rock fall probabilities were estimated based on anecdotal maintenance records, field mapping of fallen blocks, and validated with site observations and detailed structural mapping of the rock slope. Lack of detailed rock fall records, and estimates of failure likelihood of larger occurrences, required judgment to complement the available information. This was associated with increased levels of uncertainty in the calculated hazard levels. Estimating the effects of

different rock fall volumes impacting or being impacted by vehicles was also associated with uncertainty given the lack of statistical information to derive robust probabilistic models. This portion of the assessment also required judgment. Furthermore, it was recognized that rock fall occurrences showed a strong seasonality trend, and that vehicle exposure was likely to be affected by weather and visitor peaks in the area. This added further uncertainty to the interpretation of the calculated average risk values, and how risk variability was assessed.

The challenge of adopting quantitative risk assessments has been recognized and discussed previously (Ho et al. 2000) and some methods have been proposed to quantify the effect of uncertainty in the calculated risks (Macciotta et al. 2016). The method in Macciotta et al. (2016) used available information and produced plausible ranges of input variables for calculating risk, as well as their probability density functions. A Monte Carlo simulation technique was then applied to calculate the probability density function of the calculated risk. In a Monte Carlo simulation, the probability distribution of input parameters for risk calculation are used to populate a large number of calculations of risk that cover a multitude of input value combinations. The results from these calculations are then used to estimate the probability distribution of the calculated risk value. In the case presented here, the authors considered there was not enough information to develop the variables probability density functions, and therefore only the plausible range of each variable were considered. These maximum and minimum values also considered the expected fluctuation in rock fall occurrence frequency and vehicle traffic. Risk was then calculated for the expected, maximum and minimum values of the variables. The result was a range of plausible risk, which considers the effect of uncertainty in the calculations, and further acts as a proxy for risk variability.

Individual risk to highway users was found to be low, following the limited exposure of any particular individual to the study area. For the current conditions, total risk was calculated at 2.9×10^{-4} probability of fatality and a plausible total risk range between 2.0×10^{-5} and 5.5×10^{-3}. The slope protection configuration selected had a residual total risk of with a maximum range of 9.0×10^{-4}, a minimum range of 2.9×10^{-6} and a best estimate of 4.5×10^{-5}.

Risk evaluation criteria adopted corresponds to that used in Hong Kong (GEO 1998) and given the precedent of it being used in the Canadian context it was adopted for this project. The best estimate (using average values) of total risk for current conditions was found to be within tolerable thresholds, however the calculated maximum range exceeded the ALARP criteria. The slope protection configuration selected reduced the risk maximum range and best estimate within tolerable thresholds, and the minimum range within acceptable thresholds. Furthermore, it was calculated that implementation of the protective structures would improve safety by approximately one order of magnitude, which was considered adequate for the effort associated with the mitigation selected.

The case study presented here highlights the known challenge of the uncertainties associated with calculating risks associated with landslide phenomena. The paper further illustrates a way forward to provide a means for presenting a quantitative estimate of this uncertainty, such that decision-making is better informed, and safety levels are more confidently achieved. Also, calculating the relative increase in safety before and after mitigation provides increased insight for decision-making.

This case shows the importance of comprehensive and extensive records for minimizing the uncertainty in estimated hazard levels, in particular, knowledge of rock fall likelihoods as a

function of climatic condition and intensity allow for more effective risk management strategies. However, means are available for adopting quantitative risk assessments in case these records are absent or insufficient. In this regard, decision-making regarding rock fall protection always requires the designer to understand the hazard level in the area; quantitative risk assessments provide a transparent and robust framework. This case study also used and supports the precedent of the Hong Kong risk criteria being adopted by different organizations in Canada.

Acknowledgments

James Lyons (Klohn Crippen Berger) for his participation in the project, Alberta Transportation for allowing access to their information database for the study area and Alberta Environment and Parks for sharing their insights about the slope, wildlife, and human activity in the area.

References

Bonnard, C., Forlati, F., and Scavia, C. (eds). 2004. Identification and mitigation of large landslide risks in Europe—advances in risk assessment. Taylor and Francis Group plc, London, p 336

Bunce, C.M., Cruden, D.M., and Morgenstern, N.R. 1997. Assessment of the hazard from rock fall on a highway, Can Geotech J **34**:344–356

Cassidy, M.J., Uzielli, M., and Lacasse, S. 2008. Probability risk assessment of landslides: A case study at Finneidfjord. Canadian Geotechnical Journal **45**(9):1250-1267

Clague, J.J., Hungr, O., Morgenstern, N.R., and VanDine, D.F. 2015. Cheekye River (Ch'kay Stakw) and Fan Landslide Risk Tolerance Criteria (pp. 1–77). Province of British Columbia, Squamish Nation and its Partnership, and District of Squamish

Corominas, J., van Westen, C., Frattini, P., Cascini, L., Malet, J.-P., Fotopoulou, S., Catani, F., Van Den Eeckhaut, M., Mavrouli, O., Agliardi, F., Pitilakis, K., Winter, M.G., Pastor, M., Ferlisi, S., Tofani, V., Hervás, J., and Smith, J.T. 2014. Recommendations for the quantitative analysis of landslide risk. Bulletin of Engineering Geology and the Environment **73**(2):209-263

Crozier, M.J., and Glade, T. 2005. Landslide hazard and risk: issues, concepts and approach. In: Landslide hazard and risk, John Wiley and Sons, Chichester, West Sussex, UK. pg:1–40

El-Ramly, H., Morgenstern, N.R., and Cruden, D.M. 2003. Quantitative risk analysis for a cut slope. Proceedings of the Geohazards Conference 2003, Edmonton, AB. Canada

ERM-Hong Kong Ltd. 1998. Landslides and boulder falls from natural terrain: interim risk guidelines. The Government of Hong Kong Special Administrative Region. pg: 183

Fell, R., Ho, K.K.S., Lacasse, S., and Leroi, E. 2005. A framework for landslide risk assessment and management. In: Hungr, Fell, Couture, Eberhardt (eds) Landslide risk management, Proceedings of the international conference on landslide risk management. A.A. Balkema, Vancouver, pp 3–25

GEO (Geotechnical Engineering Office, Hong Kong Government). 1998. Landslides and Boulder Falls from Natural Terrain: Interim Risk Guidelines. Government of the Hong Kong Special Administrative Region, Geotechnical Engineering Office, GEO Report No.75

Google Earth Pro V 7.3.0. 2018. Canmore and area. 51°03'36.81"N 115°22'58.38"W. Image © DigitalGlobe 2018. Viewed May 6th, 2018

Government of Queensland. 2017. Vehicle Stopping Distance Information publicly available through www.qld.gov.au/transport/safety/road-safety, Accessed October 12, 2017

Health and Safety Executive (HSE). 2001. Reducing risks, protecting people. Her Majesty's Stationery Office, London, UK

Ho, K.K.S., Leroi, E., and Roberds, W.J. 2000. Quantitative risk assessment application, myths and future direction. In: GeoEng2000, Proceedings of the International Conference on Geotechnical and Geological Engineering, Melbourne, Australia. pg:269–312

Hungr, O., Clague, J.J., Morgenstern, N.R., VanDine, D.F., and Stadel, D. 2016. A review of landslide risk acceptability practices in various countries. Proceedings of the 12th International Symposium on Landslides, 12-19 June 2016, Naples, Italy

Hungr, O., Evans, S.G., and Hazzard, J. 1999. Magnitude and frequency of rock falls and rock slides along the main transportation corridors of southwestern British Columbia, Can Geotech J **36**:224–238

Klohn Crippen Berger (KCB). 2016. SITE 42 Spray Lakes Rockfall - Preliminary Design Report (Draft). Submitted to Alberta Transportation in September 2, 2016

Kong, W.K. 2002. Risk assessment of slopes. Q J Eng Geol Hydrogeol **35**:213–222

Lacasse, S., Eidsvik, U., Nadim, F., Høeg, K., and Blikra, L.H. 2008. Event tree analysis of Aknes Rockslide hazard, Proceedings of the 4th Canadian Conference on Geohazards: from Causes to management, Canadian Geotechnical Society, QuebecCity, QB, Canada pg:551–557

Lan, H., Martin, C.D., and Lim, C.H. 2007. Rock fall analyst: a GIS extension for three-dimensional and spatially distributed rock fall hazard model- ing. Comput Geosci **33**:262–279

Lan, H., Martin, C.D., Zhou, C., and Lim, C.H. 2010 Rock fall hazard analysis using LiDAR and spatial modeling. Geomorphology **118**:213–223

Lu, P., Catani, F., Tofani, V., and Casagli, N. 2014. Quantitative hazard and risk assessment for slow-moving landslides from Persistent Scatterer Interferometry. Landslides **11**(4):685–696

Macciotta, R., Cruden, D.M., Martin, C.D., and Morgenstern, N.R. 2011. Combining geology, morphology and 3D modelling to understand the rock fall distribution along the railways in the Fraser River Valley, between Hope and Boston Bar, In: Eberhardt, E., and Stead, D. (eds), Slope Stability 2011: Proceedings of the 2011 International Symposium on Rock Slope Stability in Open Pit Mining and Civil Engineering, 18–21 September 2011, Vancouver, BC, Canada

Macciotta, R., Hendry, M., Cruden, D.M., Blais-Stevens, A., and Edwards, T. 2017a. Quantifying rock fall probabilities and their temporal distribution associated with weather seasonality. Landslides **14**(6):2025-2039

Macciotta, R., and Martin, C.D. 2013. Role of 3D Topography in Rock Fall Trajectories and Model Sensitivity to Input Parameters. In L. J. Pyrak-Nolte et al. (eds.) 47th US Rock Mechanics/Geomechanics Symposium. San Francisco, California, USA, 23 - 26 June, 2013. pp:1–9

Macciotta, R., and Martin, C.D. 2015. Remote Structural Mapping and Discrete Fracture Networks to Calculate Rockfall Volumes at Tornado Mountain, British Columbia. In: 49th US Rock Mechanics/Geomechanics Symposium, San Francisco, CA, US, pp:9

Macciotta, R., Martin, C.D., Cruden, D.M., Hendry, M., and Edwards, T. 2017b. Rock fall hazard control along a section of railway based on quantified risk. Georisk **11**(3):272-284

Macciotta, R., Martin, C.D., Morgenstern, N.R., and Cruden, D.M. 2016. Quantitative risk assessment of slope hazards along a section of railway in the Canadian Cordillera—a methodology considering the uncertainty in the results. Landslides **13**(1): 115–127

Macciotta, R., Gräpel, C., Duxbury, J., Keegan, T.R., and Skirrow, R. 2018. Explicit estimation of rock slope failure likelihood for hazard assessment and safety engineering near Canmore, AB. In: Proceedings of the 7th Canadian Conference on Geohazards: Geohazards7, Canadian Geotechnical Society, Canmore, Alberta, Canada, June 3 to 6, 2018 pp:9

Morgenstern, N.R. 1997. Toward landslide risk assessment in practice. In: Cruden and Fell (eds.) Landslide Risk Assessment, Proceedings of the International Workshop on Landslide Risk Assessment, Hawaii. A.A. Balkema. pp:15–23

Mostyn, G., and Sullivan, T. 2002. Quantitative risk assessment of the Thredbo landslide. Aust Geomech **37**(2):169–181

Price, R.A. 1970. Geology, Canmore (west half), west of Fifth Meridian, Alberta. Geological Survey of Canada, "A" Series Map 1266A (1:50,000)

Richards, D.C. 2010. Relationship between speed and risk of fatal injury: Pedestrians and car occupants. Transport Research Laboratory, London, UK

Rocscience Inc. 2013. RocFall version 4.058, http://www.rocscience.com

Rodriguez, J.L., Macciotta, R., Hendry, M., Edwards, T., and Evans, T. 2017. Slope hazards and risk engineering in the Canadian railway network through the Cordillera. In: DellAcqua, G., and Wegman, F. (eds.) Transport Infrastructure and Systems, Rome, April 10 – 12, 2017. Taylor & Francis Group, London, pg:163-168

Statistics Canada. 2012. Mortality, Summary List of Causes 2009. Catalogue no. 84F0209X. http://www.statcan.gc.ca. Accessed May 05, 2017

Uzielli, M., Catani, F., Tofani, V., and Casagli, N. 2015. Risk analysis for the Ancona landslide—II: estimation of risk to buildings. Landslides **12**(1):83-100

VanDine, D.F. 2018. Evolution of Landslide Hazard and Risk Assessments in Canada. In: Proceedings of the 7th Canadian Conference on Geohazards: Geohazards7, Canadian Geotechnical Society, Canmore, Alberta, Canada, June 3 to 6, 2018 pp:20

Vranken, L., Vantilt, G., Van Den Eeckhaut, M., Vandekerckhove, L., and Poesen, J. 2015. Landslide risk assessment in a densely populated hilly area. Landslides **12**(4):787-798

List of figures:

Figure 9 Cross sections selected for trajectory modelling of falling blocks (a) and rock fall trajectory model output for existing conditions for Cross Section 3 (b) (modified from Macciotta et al. 2018)

Figure 10 Event tree for consequence quantification

Figure 11 Probability of fatality for car drivers at different speeds (after Richards 2010). Solid line represents the best estimate. The confidence interval for 95% of estimates is represented between dashed lines

Figure 12 Average total risk associated with rock slope failures at the S042 site

Figure 13 Highest (a) and Lowest (b) risk scenarios associated with a rock slope failure the S042 site

Figure 14 Average (a) Highest (b) and Lowest (c) individual risk scenarios associated with failure at the S042 site

Figure 15 Estimated total (a) and individual (b) risk to highway users at the S042 site and plausible ranges. Mortality rates in Canada and criteria proposed for Hong Kong and the HSE in the UK are shown for benchmark

Figure 16 Estimated total (a) and individual (b) residual risk to highway users at the S042 site and plausible ranges. Mortality rates in Canada and criteria proposed for Hong Kong and the HSE in the UK are shown for benchmark

Table 1 Discontinuity characteristics (Macciotta et al. 2018)

Disc. Set	Type	Dip (°)	Dip Direction (°)
J1	Joint	80	149
J2	Joint	59	25
J2b	Joint	46	77
J4	Shear	58	248
S0	Bedding	38	252

Disc. Set	Trace length (m)		
	Min.	Max.	Mean
J1	0.4	3.0	1.1
J2	0.3	3.0	1.1
J2b	0.5	1.3	0.9
J4	0.4	2.5	0.8
So	Continuous		

Disc. Set	Spacing (m)		
	Min.	Max.	Mean
J1	0.1	2.4	0.5
J2	0.1	2.8	1.0
J2b	0.04	0.2	0.1
J4	N/A		
So	0.1	0.4	0.3

Table 2 Area and number of blocks surveyed (Macciotta et al. 2018)

Window	Area (m^2)	No. of blocks surveyed
1	50	17
2	44	12
3	62	23
4	Linear scan	76
5	40	33
6	80	14
7	80	20
Total	-	195

Table 3 Estimated frequency of block volumes reaching the highway

Failure volume (m^3)	Estimated frequency	Justification
Less than 0.1 m^3	90	Relative cumulative frequency scaled to estimated number of blocks reaching the highway. Surveyed data extrapolated to 1 m^3. Data driven and minor extrapolation.
0.1 to 0.5 m^3	10	
0.5 to 1 m^3	0.2	
1 to 10 m^3	0.1 (one every 10 years)	equivalent to one 1 m^3 to 2.15 m^3 block. Based on extrapolation of the cumulative frequency and experienced opinion. frequency can be conservative given the history of the site (one occurrence in recent history).
10 to 100 m^3	0.01 (one every 100 years) or less	Much uncertainty associated with this estimate. Based on extrapolation of the cumulative frequency and experienced opinion. Large blocks embedded on talus suggest disaggregated blocks from large failures would tend to stop before reaching the highway and minimize the volume with the potential to block it.
Larger slope instabilities (up to 1000 m^3)	Uncertain. Up to 0.01 annual probability for risk assessment purposes.	Much uncertainty associated with this estimate. Based on experienced opinion. Large blocks embedded on talus suggest disaggregated blocks from large failures would tend to stop before reaching the highway and minimize the volume with the potential to block it. Probability adopted for risk assessment purposes correspond to levels of disaggregation of some large blocks in Sectors A, B and D. Extrapolating the survey data is not considered adequate for these volumes.

Table 4 Input surface parameters used for the 2-dimensional trajectory simulations

Input Parameter	Hard Rock Surface		Talus Surface	
	Mean	Standard Deviation	Mean	Standard Deviation
Normal Coefficient of Restitution, Rn	0.40	0.04	0.30	0.04
Tangential Coefficient of Restitution, Rt	0.85	0.04	0.70	0.04
Friction Angle	15	2	20	2

Table 5 Probability that falling blocks/debris coincide with vehicle – $P[Sm]$

Estimated:	L (km)	C	V (km/h)	$P[Sm]$
Absolute upper bound	0.006	3000	40	1.9×10^{-2}
Upper bound used	0.006	3000	70	1.1×10^{-2}
Absolute lower bound	0.004	500	70	1.2×10^{-3}
Lower bound used	0.004	500	40	2.1×10^{-3}
Average	0.005	1260	60	4.4×10^{-3}

Table 6 Probability that falling blocks/debris and moving vehicle are in the same lane - $P[Sw]$

Failure volume group (m^3)	$P[Sw]$	Justification
Less than 0.1 m^3	0.05	Rockfall trajectory models and observations suggest most blocks reach the highway near the toe of the talus slope. It is assumed that half the daily traffic would be at the farthest lane from the toe (0.5 chance of not coinciding on the same side of the road). A large percentage of modelled blocks impact at the toe of the talus slope or at the auxiliary area of the highway and would travel onto the highway at low velocities and heights (therefore missing the vehicle or impacting the tires). A conservative chance of one in 20 occurrences was adopted for calculation (0.05).
0.1 to 0.5 m^3	0.05	
0.5 to 1 m^3	0.1	Same observations as above. These blocks have larger dimensions than the other two groups, therefore a conservative chance of one in 10 occurrences was adopted for calculation (0.1).
1 to 10 m^3	0.25	Same observations as above, however, due to the larger dimensions, a conservative chance that one of every four occurrences was adopted for calculation (0.25).
10 to 100 m^3	0.5	Same observations as above, however due to the large volumes it is assumed that the failure will cover one whole lane.
Larger slope instabilities (up to 1000 m^3)	1	These volumes have the potential to impact the entire width of the highway.

Table 7 Probability of fatality given a vehicle gets impacted by falling blocks/debris - $P[F-fb]$

Failure volume group (m^3)	$P[F-fb]$	Justification
Less than 0.1 m^3	Very unlikely (1 in a hundred, 0.001, for calculation purposes)	Small block when compared to vehicle. Impact would need to occur at the area of occupancy, pierce the skin of the vehicle, and hit the occupant at critical location. Models show most blocks reach the highway at low heights. Fatality under this scenario is assumed very unlikely.
0.1 to 0.5 m^3	0.01	Block dimensions smaller than 1/3 of vehicle dimensions. Impact would need to occur at or near the area of occupancy inside the vehicle or cause loss of control. Fatality is assumed unlikely.
0.5 to 1 m^3	0.1	Similar as above, however block about 1/3 of vehicle dimension would make critical impact more likely. A plausible chance of one in ten occurrences was considered adequately conservative.
1 to 10 m^3	0.5	Block dimensions about 1/3 to 2/3 of vehicle dimensions. An even chance probability (0.5) was considered adequately conservative.
10 to 100 m^3	1	Large volume relative to vehicle size. Perceived likelihood of serious impact to occupants is large under this scenario. Maximum probability (1) is adopted (conservative).
Larger slope instabilities (up to 1000 m^3)	1	

Table 8 Vehicle stopping distances (including driver reaction distance) after Government of Queensland (2017)

Vehicle speed (km/h)	Stopping distance
40	up to 30m
60	up to 54m
70	up to 69m

Table 9 Adopted P[i] and their justification

Failure volume group (m^3)	$P[i]$	Justification
Less than 0.1 m^3	Negligible	Very small blocks easily cleared by the height of most vehicles or avoided by minimum manoeuvring.
0.1 to 0.5 m^3	0.01	Considering highway width to block size, manoeuvring area is wide. Observations and models indicate material likely block the auxiliary section of highway, its shoulder or adjacent lane. Small blocks would be easily avoided by minimum manoeuvring. Sight distance is enough for vehicles to stop or significantly decelerate. Probability of impact is considered extremely low. If impacted, it is expected a very low speed.
0.5 to 1 m^3	0.02	Same as above, however larger blocks would increase the impact probability but still considered very low. Conservative chance of one in one 50 occurrences was adopted.
1 to 10 m^3	0.02	
10 to 100 m^3	0.05	Same as above, however larger blocks would increase the impact probability but still considered low. Conservative chance of one in 20 occurrences was adopted.
Larger slope instabilities (up to 1000 m^3)	0.1	Vehicles likely to stop before impact. Conservatively assumed a chance of one in ten that the vehicle will come in contact with debris, however at low speed.

Table 10 Probability of fatality at representative speeds along the S042 site and half the speed (according to Figure 11)

	Speed (km/h)	Prob.	Half speed (km/h)	Prob.
Upper bound	70	0.3	35	Low (approximated to 1% or 0.01)
Lower bound	40	0.01	20	Very unlikely (approximated to 0.1% or 0.001)
Average	60	0.1	30	Very unlikely (approximated to 0.1% or 0.001)

Table 11 Probability of fatality given vehicle impacts a blocked section of highway - $P[F-bh]$

Failure volume group (m^3)	$P[F-bh]$	Justification
Less than 0.1 m^3	Negligible	If vehicle impacted at highway speed (distracted driver), likely minor vehicle damage (small block).
0.1 to 0.5 m^3	0.001	Extremely low probability of fatality considering material volume and expected speed reduction before impact. Value adopted for calculation.
0.5 to 1 m^3	0.001	
1 to 10 m^3	0.001	
10 to 100 m^3	0.01	Similar as above with increased probability due to larger volume and considering potential inadequate reaction of driver (not decelerating).
Larger slope instabilities (up to 1000 m^3)	0.01	

Table 12 Elicited probability of catchment for the proposed protection

Block volume group (m^3)	% capture 6m high, 3000 KJ catch fence and hanging wire mesh curtain at zones D and E	Justification
Less than 0.1 m^3	99%	Fence and curtain will effectively intercept the blocks. Energy specifications for the fence at the toe will contain the falling block volume at high velocities suggested by the model.
0.1 to 0.5 m^3	99%	
0.5 to 1 m^3	99%	
1 to 10 m^3	75%	Fence and curtain will effectively intercept the blocks. Energy specifications for the fence at the toe will contain the disaggregated falling blocks at lower velocities. It is expected the talus slope to act as effective energy attenuator for the larger blocks. Justified by observations of 1 to 3 m (equivalent size) blocks embedded in the talus slope. Adopting a chance of 75% was considered adequate.
10 to 100 m^3	30%	Same as above. A conservative 30% chance that blocks will be contained is adopted for larger volumes.
Larger slope instabilities (up to 1000 m^3)	0%	Conservative assumption that the fence will not stop these volumes.

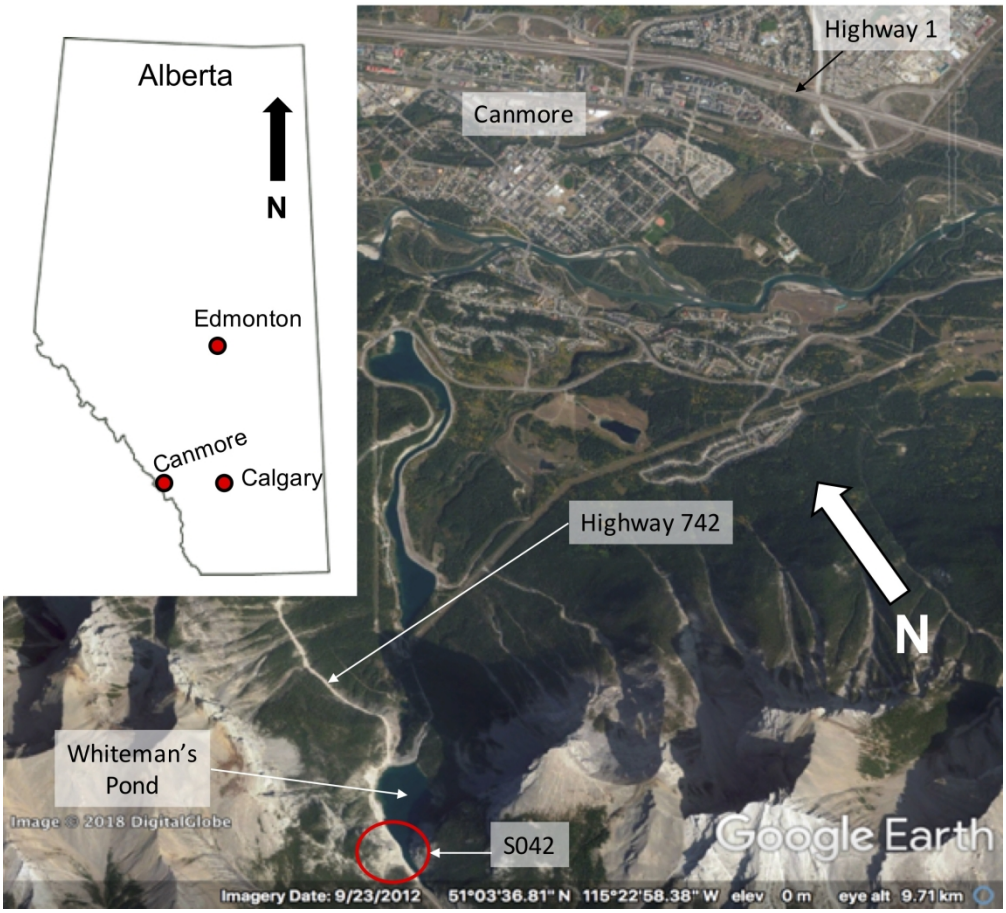

Figure 1 Location of the S042 site. Base image after Google Earth (2018) (Modified from Macciotta et al. 2018)

211x191mm (300 x 300 DPI)

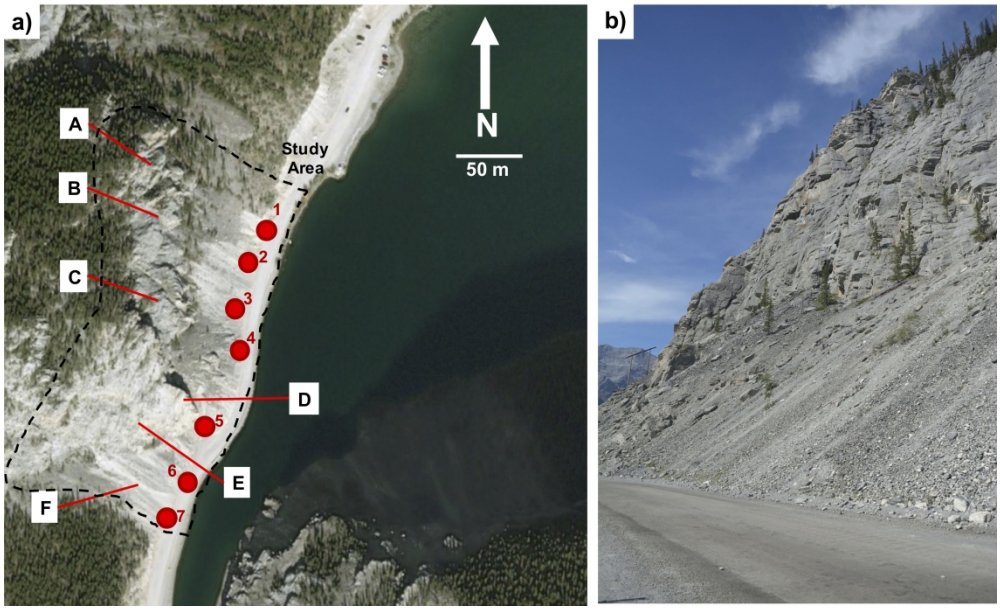

Figure 2 Plan view of the S042 site showing Sectors A through F for reference and rock debris window mapping Locations 1 through 7 (a). Photograph of Sector D taken from Location 1 (Modified from Macciotta et al. 2018)

297x183mm (300 x 300 DPI)

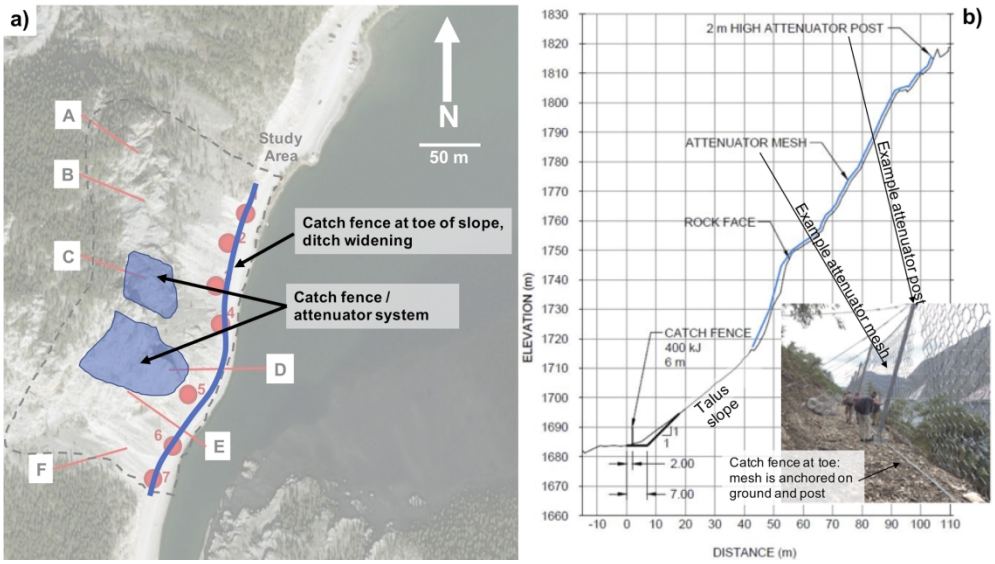

Figure 3 Location of the catch fence and ditch at the toe of the S042 site and attenuator-curtain system (a). Cross section in Sector C (red line in Sector C) showing location of attenuator mesh, the catch fence and ditch, and illustrative example of system with 6 m high posts (photo by the first author and modified from Rodriguez et al. 2017) (b)

182x104mm (300 x 300 DPI)

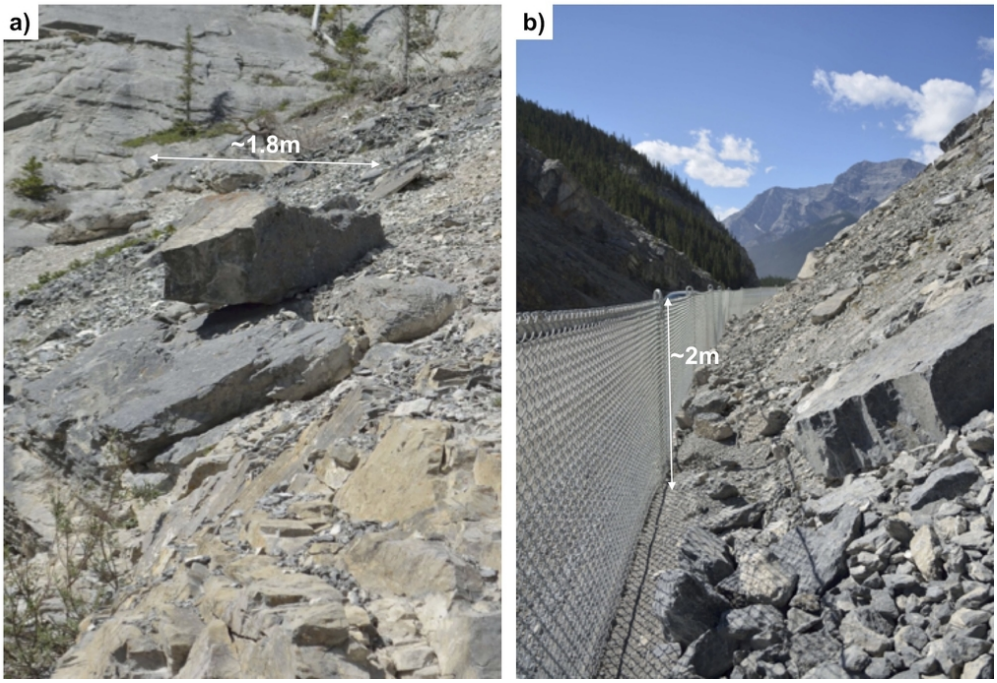

Figure 4 Rock blocks larger than 1 m3 contained within the talus slope at sector C (a) and adjacent to the road at sector D (b)

85x58mm (300 x 300 DPI)

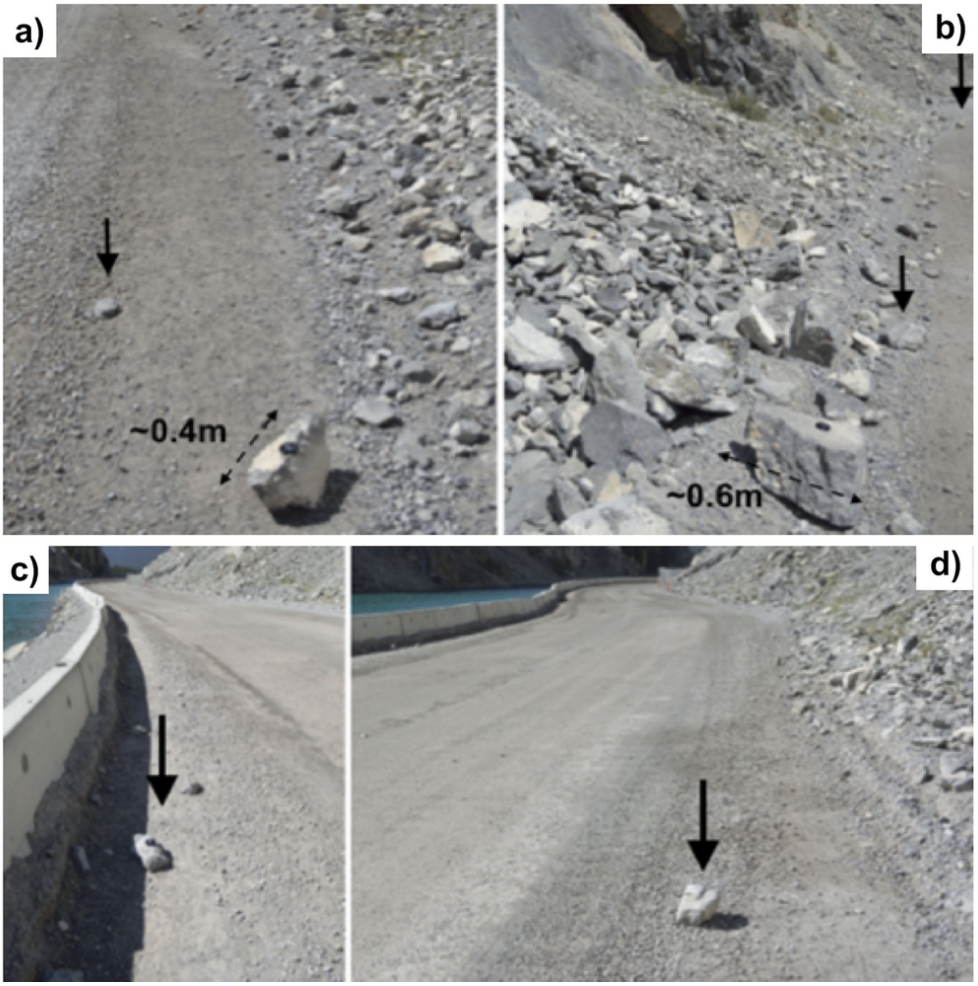

Figure 5 Fallen blocks at the toe of the talus slope in sector F (a, b), adjacent to the road at the lake side (c), and at the toe of the talus slope in Sector B (d) (after Macciotta et al. 2018)

85x84mm (300 x 300 DPI)

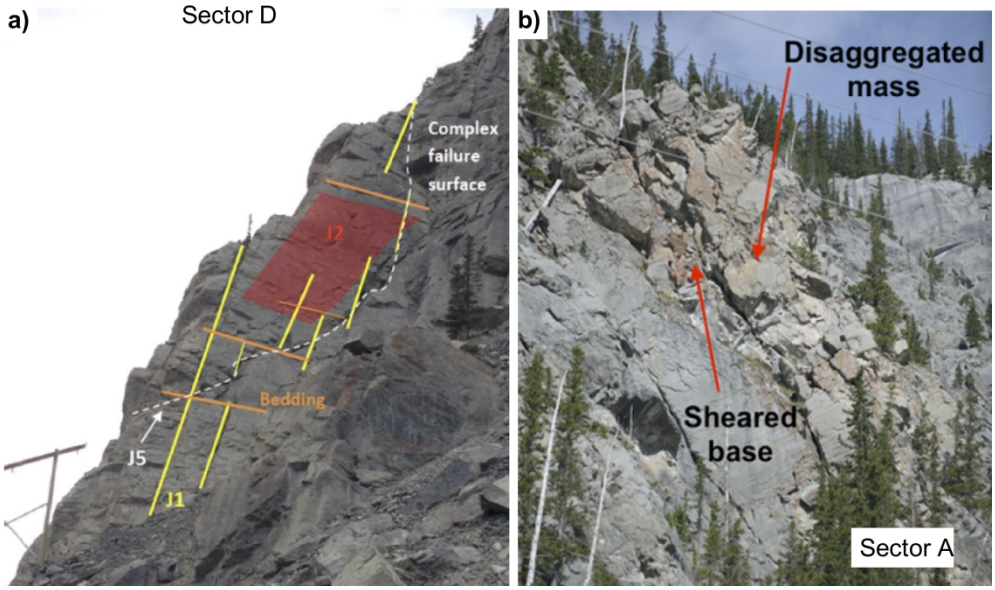

Figure 6 Evidence of progressive failure mechanisms (after Macciotta et al. 2018)

285x169mm (300 x 300 DPI)

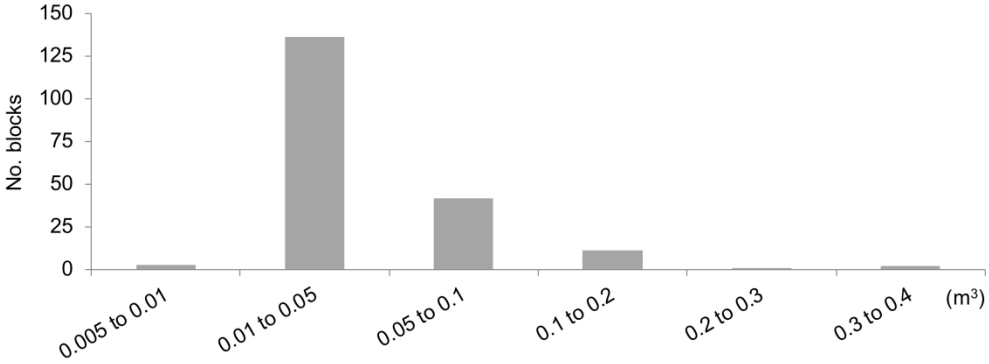

Figure 7 Histogram of surveyed block volumes (after Macciotta et al. 2018)

338x129mm (300 x 300 DPI)

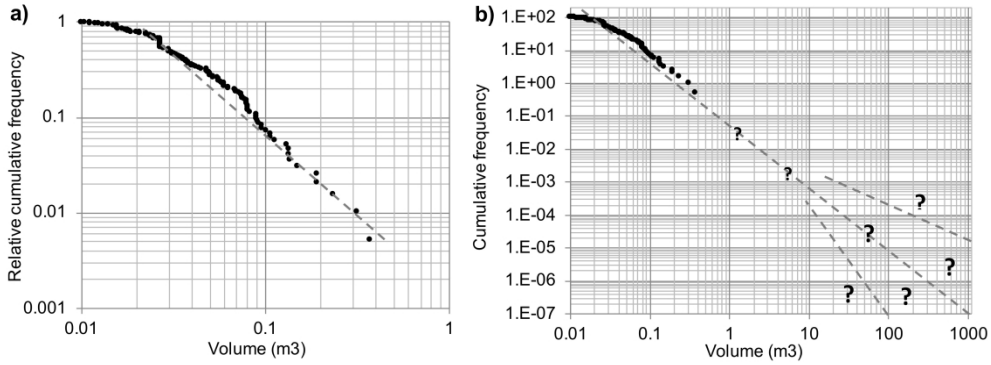

Figure 8 Relative (a) and absolute (b) cumulative frequency of surveyed blocks. 100 blocks was used as anchor point in (b) for calculating the absolute rock fall frequency (1.E+02 for a volume of 0.01 m3) (modified from Macciotta et al. 2018)

326x120mm (300 x 300 DPI)

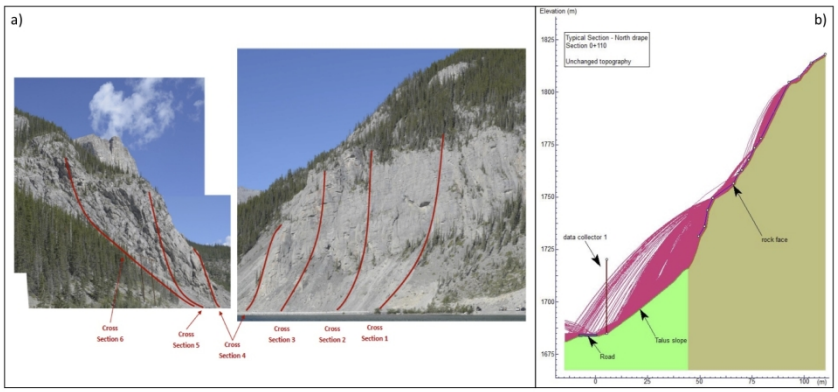

Figure 9 Cross sections selected for trajectory modelling of falling blocks (a) and rock fall trajectory model output for existing conditions for Cross Section 3 (b) (modified from Macciotta et al. 2018)

199x94mm (300 x 300 DPI)

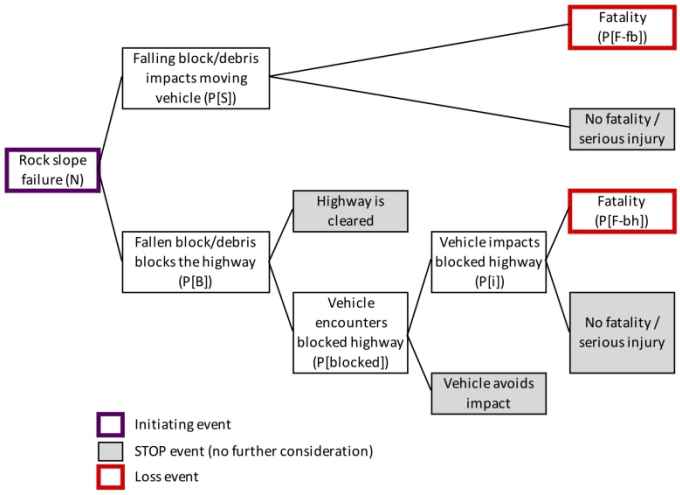

Figure 10 Event tree for consequence quantification

249x175mm (300 x 300 DPI)

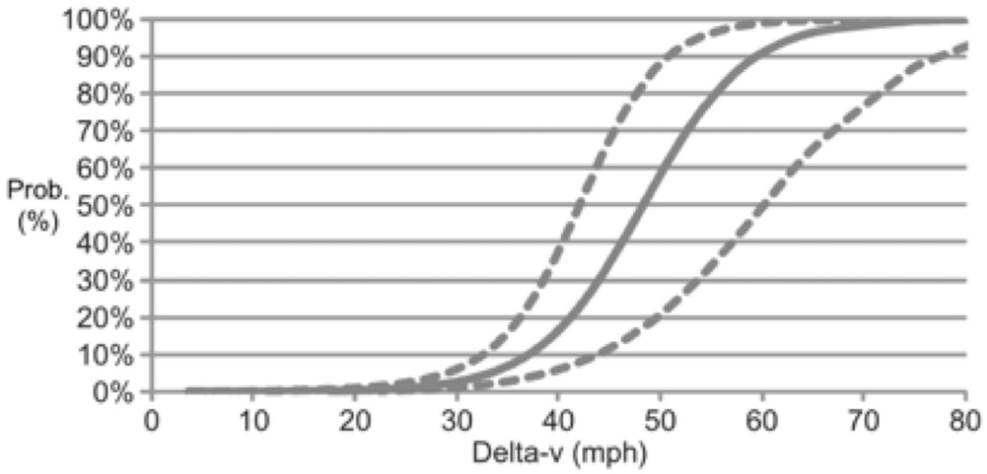

Figure 11 Probability of fatality for car drivers at different speeds (after Richards 2010)

85x40mm (300 x 300 DPI)

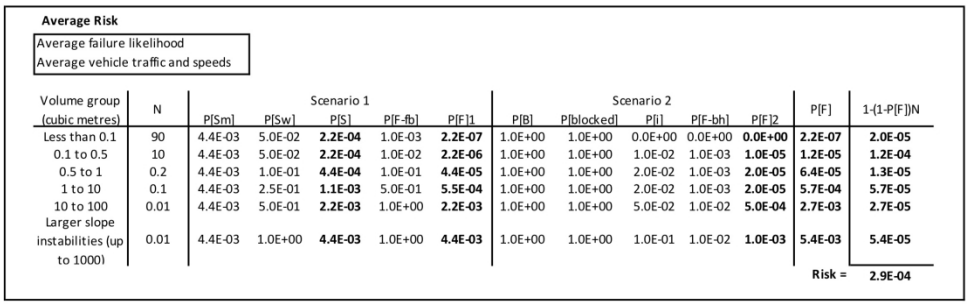

Average Risk

Average failure likelihood
Average vehicle traffic and speeds

Volume group (cubic metres)	N	Scenario 1					Scenario 2					P[F]	1-(1-P[F])N
		P[Sm]	P[Sw]	P[S]	P[F-fb]	P[F]1	P[B]	P[blocked]	P[i]	P[F-bh]	P[F]2		
Less than 0.1	90	4.4E-03	5.0E-02	**2.2E-04**	1.0E-03	**2.2E-07**	1.0E+00	1.0E+00	0.0E+00	0.0E+00	**0.0E+00**	**2.2E-07**	**2.0E-05**
0.1 to 0.5	10	4.4E-03	5.0E-02	**2.2E-04**	1.0E-02	**2.2E-06**	1.0E+00	1.0E+00	1.0E-02	1.0E-03	**1.0E-05**	**1.2E-05**	**1.2E-04**
0.5 to 1	0.2	4.4E-03	1.0E-01	**4.4E-04**	1.0E-01	**4.4E-05**	1.0E+00	1.0E+00	2.0E-02	1.0E-03	**2.0E-05**	**6.4E-05**	**1.3E-05**
1 to 10	0.1	4.4E-03	2.5E-01	**1.1E-03**	5.0E-01	**5.5E-04**	1.0E+00	1.0E+00	2.0E-02	1.0E-03	**2.0E-05**	**5.7E-04**	**5.7E-05**
10 to 100	0.01	4.4E-03	5.0E-01	**2.2E-03**	1.0E+00	**2.2E-03**	1.0E+00	1.0E+00	5.0E-02	1.0E-02	**5.0E-04**	**2.7E-03**	**2.7E-05**
Larger slope instabilities (up to 1000)	0.01	4.4E-03	1.0E+00	**4.4E-03**	1.0E+00	**4.4E-03**	1.0E+00	1.0E+00	1.0E-01	1.0E-02	**1.0E-03**	**5.4E-03**	**5.4E-05**
												Risk =	**2.9E-04**

Figure 12 Average total risk associated with rock slope failures at the S042 site

202x68mm (300 x 300 DPI)

a) Highest risk scenario

10 times failure likelihood
Max. vehicle traffic and speeds

Volume group (cubic metres)	N	Scenario 1					Scenario 2					P[F]	1-(1-P[F])N
		P[Sm]	P[Sw]	P[S]	P[F-fb]	P[F]1	P[B]	P[blocked]	P[i]	P[F-bh]	P[F]2		
Less than 0.1	900	1.1E-02	5.0E-02	**5.5E-04**	1.0E-03	**5.5E-07**	1.0E+00	1.0E+00	0.0E+00	0.0E+00	**0.0E+00**	**5.5E-07**	**4.9E-04**
0.1 to 0.5	100	1.1E-02	5.0E-02	**5.5E-04**	1.0E-02	**5.5E-06**	1.0E+00	1.0E+00	1.0E-02	1.0E-03	**1.0E-05**	**1.6E-05**	**1.5E-03**
0.5 to 1	2	1.1E-02	1.0E-01	**1.1E-03**	1.0E-01	**1.1E-04**	1.0E+00	1.0E+00	2.0E-02	1.0E-03	**2.0E-05**	**1.3E-04**	**2.6E-04**
1 to 10	1	1.1E-02	2.5E-01	**2.8E-03**	5.0E-01	**1.4E-03**	1.0E+00	1.0E+00	2.0E-02	1.0E-03	**2.0E-05**	**1.4E-03**	**1.4E-03**
10 to 100	0.1	1.1E-02	5.0E-01	**5.5E-03**	1.0E+00	**5.5E-03**	1.0E+00	1.0E+00	5.0E-02	1.0E-02	**5.0E-04**	**6.0E-03**	**6.0E-04**
Larger slope instabilities (up to 1000)	0.1	1.1E-02	1.0E+00	**1.1E-02**	1.0E+00	**1.1E-02**	1.0E+00	1.0E+00	1.0E-01	1.0E-02	**1.0E-03**	**1.2E-02**	**1.2E-03**
												Risk =	**5.5E-03**

b) Lowest risk scenario

1/10 failure likelihood
Min. vehicle traffic and speeds

Volume group (cubic metres)	N	Scenario 1					Scenario 2					P[F]	1-(1-P[F])N
		P[Sm]	P[Sw]	P[S]	P[F-fb]	P[F]1	P[B]	P[blocked]	P[i]	P[F-bh]	P[F]2		
Less than 0.1	9	2.1E-03	5.0E-02	**1.1E-04**	1.0E-03	**1.1E-07**	1.0E+00	1.0E+00	0.0E+00	0.0E+00	**0.0E+00**	**1.1E-07**	**9.4E-07**
0.1 to 0.5	1	2.1E-03	5.0E-02	**1.1E-04**	1.0E-02	**1.1E-06**	1.0E+00	1.0E+00	1.0E-02	1.0E-03	**1.0E-05**	**1.1E-05**	**1.1E-05**
0.5 to 1	0.02	2.1E-03	1.0E-01	**2.1E-04**	1.0E-01	**2.1E-05**	1.0E+00	1.0E+00	2.0E-02	1.0E-03	**2.0E-05**	**4.1E-05**	**8.2E-07**
1 to 10	0.01	2.1E-03	2.5E-01	**5.3E-04**	5.0E-01	**2.6E-04**	1.0E+00	1.0E+00	2.0E-02	1.0E-03	**2.0E-05**	**2.8E-04**	**2.8E-06**
10 to 100	0.001	2.1E-03	5.0E-01	**1.1E-03**	1.0E+00	**1.1E-03**	1.0E+00	1.0E+00	5.0E-02	1.0E-02	**5.0E-04**	**1.6E-03**	**1.6E-06**
Larger slope instabilities (up to 1000)	0.001	2.1E-03	1.0E+00	**2.1E-03**	1.0E+00	**2.1E-03**	1.0E+00	1.0E+00	1.0E-01	1.0E-02	**1.0E-03**	**3.1E-03**	**3.1E-06**
												Risk =	**2.0E-05**

Figure 13 Highest (a) and Lowest (b) risk scenarios associated with a rock slope failure the S042 site

202x122mm (300 x 300 DPI)

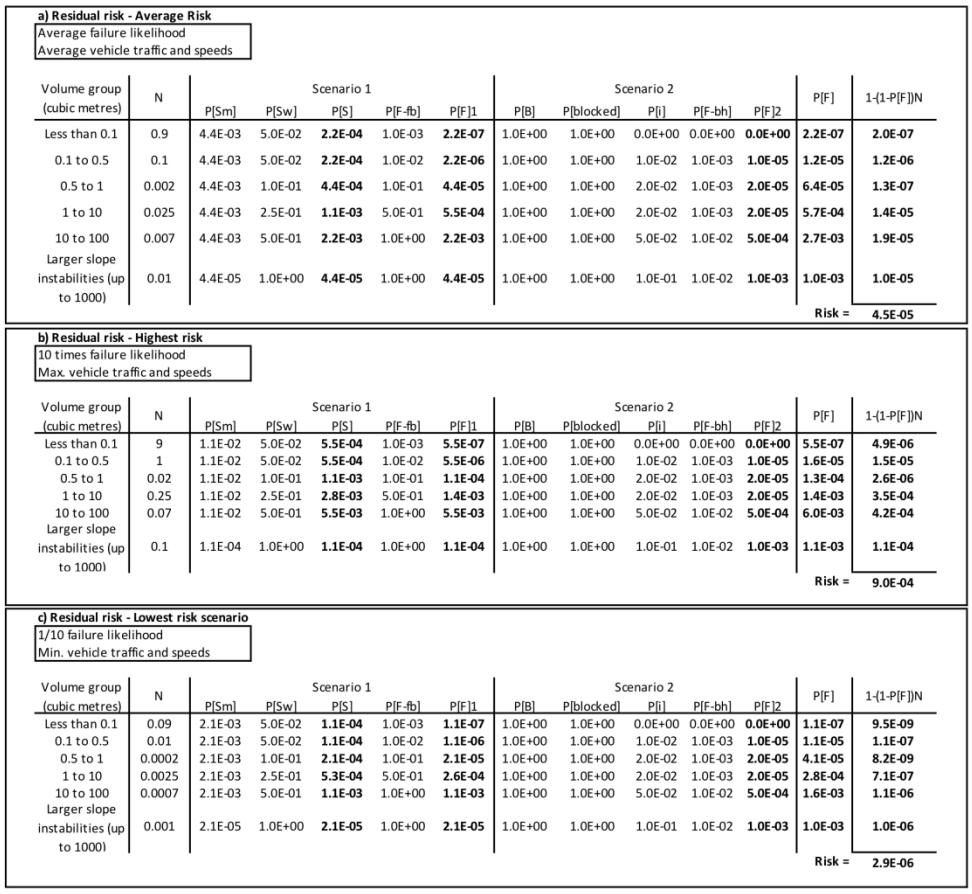

a) Residual risk - Average Risk

Average failure likelihood
Average vehicle traffic and speeds

Volume group (cubic metres)	N	Scenario 1					Scenario 2					P[F]	1-(1-P[F])N
		P[Sm]	P[Sw]	P[S]	P[F-fb]	P[F]1	P[B]	P[blocked]	P[i]	P[F-bh]	P[F]2		
Less than 0.1	0.9	4.4E-03	5.0E-02	**2.2E-04**	1.0E-03	**2.2E-07**	1.0E+00	1.0E+00	0.0E+00	0.0E+00	**0.0E+00**	**2.2E-07**	**2.0E-07**
0.1 to 0.5	0.1	4.4E-03	5.0E-02	**2.2E-04**	1.0E-02	**2.2E-06**	1.0E+00	1.0E+00	1.0E-02	1.0E-03	**1.0E-05**	**1.2E-05**	**1.2E-06**
0.5 to 1	0.002	4.4E-03	1.0E-01	**4.4E-04**	1.0E-01	**4.4E-05**	1.0E+00	1.0E+00	2.0E-02	1.0E-03	**2.0E-05**	**6.4E-05**	**1.3E-07**
1 to 10	0.025	4.4E-03	2.5E-01	**1.1E-03**	5.0E-01	**5.5E-04**	1.0E+00	1.0E+00	2.0E-02	1.0E-03	**2.0E-05**	**5.7E-04**	**1.4E-05**
10 to 100	0.007	4.4E-03	5.0E-01	**2.2E-03**	1.0E+00	**2.2E-03**	1.0E+00	1.0E+00	5.0E-02	1.0E-02	**5.0E-04**	**2.7E-03**	**1.9E-05**
Larger slope instabilities (up to 1000)	0.01	4.4E-05	1.0E+00	**4.4E-05**	1.0E+00	**4.4E-05**	1.0E+00	1.0E+00	1.0E-01	1.0E-02	**1.0E-03**	**1.0E-03**	**1.0E-05**
												Risk =	**4.5E-05**

b) Residual risk - Highest risk

10 times failure likelihood
Max. vehicle traffic and speeds

Volume group (cubic metres)	N	Scenario 1					Scenario 2					P[F]	1-(1-P[F])N
		P[Sm]	P[Sw]	P[S]	P[F-fb]	P[F]1	P[B]	P[blocked]	P[i]	P[F-bh]	P[F]2		
Less than 0.1	9	1.1E-02	5.0E-02	**5.5E-04**	1.0E-03	**5.5E-07**	1.0E+00	1.0E+00	0.0E+00	0.0E+00	**0.0E+00**	**5.5E-07**	**4.9E-06**
0.1 to 0.5	1	1.1E-02	5.0E-02	**5.5E-04**	1.0E-02	**5.5E-06**	1.0E+00	1.0E+00	1.0E-02	1.0E-03	**1.0E-05**	**1.6E-05**	**1.5E-05**
0.5 to 1	0.02	1.1E-02	1.0E-01	**1.1E-03**	1.0E-01	**1.1E-04**	1.0E+00	1.0E+00	2.0E-02	1.0E-03	**2.0E-05**	**1.3E-04**	**2.6E-06**
1 to 10	0.25	1.1E-02	2.5E-01	**2.8E-03**	5.0E-01	**1.4E-03**	1.0E+00	1.0E+00	2.0E-02	1.0E-03	**2.0E-05**	**1.4E-03**	**3.5E-04**
10 to 100	0.07	1.1E-02	5.0E-01	**5.5E-03**	1.0E+00	**5.5E-03**	1.0E+00	1.0E+00	5.0E-02	1.0E-02	**5.0E-04**	**6.0E-03**	**4.2E-04**
Larger slope instabilities (up to 1000)	0.1	1.1E-04	1.0E+00	**1.1E-04**	1.0E+00	**1.1E-04**	1.0E+00	1.0E+00	1.0E-01	1.0E-02	**1.0E-03**	**1.1E-03**	**1.1E-04**
												Risk =	**9.0E-04**

c) Residual risk - Lowest risk scenario

1/10 failure likelihood
Min. vehicle traffic and speeds

Volume group (cubic metres)	N	Scenario 1					Scenario 2					P[F]	1-(1-P[F])N
		P[Sm]	P[Sw]	P[S]	P[F-fb]	P[F]1	P[B]	P[blocked]	P[i]	P[F-bh]	P[F]2		
Less than 0.1	0.09	2.1E-03	5.0E-02	**1.1E-04**	1.0E-03	**1.1E-07**	1.0E+00	1.0E+00	0.0E+00	0.0E+00	**0.0E+00**	**1.1E-07**	**9.5E-09**
0.1 to 0.5	0.01	2.1E-03	5.0E-02	**1.1E-04**	1.0E-02	**1.1E-06**	1.0E+00	1.0E+00	1.0E-02	1.0E-03	**1.0E-05**	**1.1E-05**	**1.1E-07**
0.5 to 1	0.0002	2.1E-03	1.0E-01	**2.1E-04**	1.0E-01	**2.1E-05**	1.0E+00	1.0E+00	2.0E-02	1.0E-03	**2.0E-05**	**4.1E-05**	**8.2E-09**
1 to 10	0.0025	2.1E-03	2.5E-01	**5.3E-04**	5.0E-01	**2.6E-04**	1.0E+00	1.0E+00	2.0E-02	1.0E-03	**2.0E-05**	**2.8E-04**	**7.1E-07**
10 to 100	0.0007	2.1E-03	5.0E-01	**1.1E-03**	1.0E+00	**1.1E-03**	1.0E+00	1.0E+00	5.0E-02	1.0E-02	**5.0E-04**	**1.6E-03**	**1.1E-06**
Larger slope instabilities (up to 1000)	0.001	2.1E-05	1.0E+00	**2.1E-05**	1.0E+00	**2.1E-05**	1.0E+00	1.0E+00	1.0E-01	1.0E-02	**1.0E-03**	**1.0E-03**	**1.0E-06**
												Risk =	**2.9E-06**

Figure 14 Average (a) Highest (b) and Lowest (c) individual risk scenarios associated with failure at the S042 site

202x185mm (300 x 300 DPI)

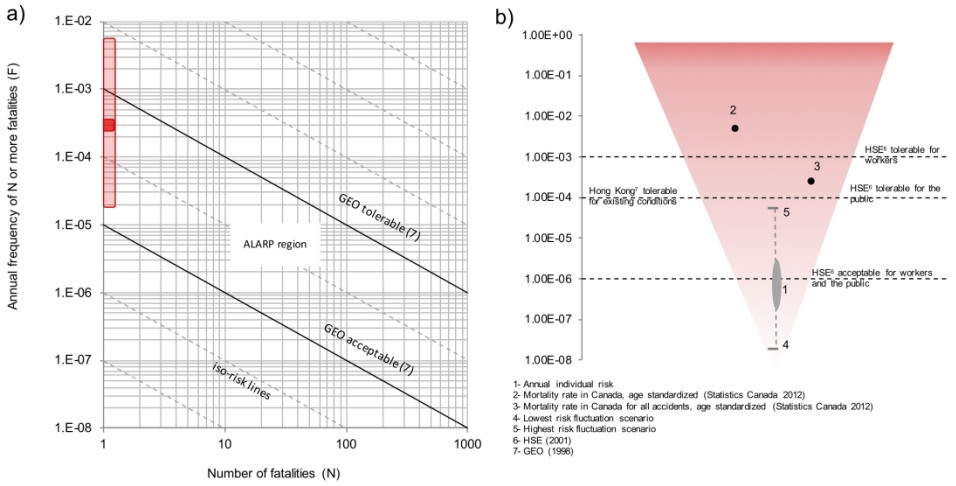

Figure 15 Estimated total (a) and individual (b) risk to highway users at the S042 site and plausible ranges. Mortality rates in Canada and criteria proposed for Hong Kong and the HSE in the UK are shown for benchmark

301x151mm (300 x 300 DPI)

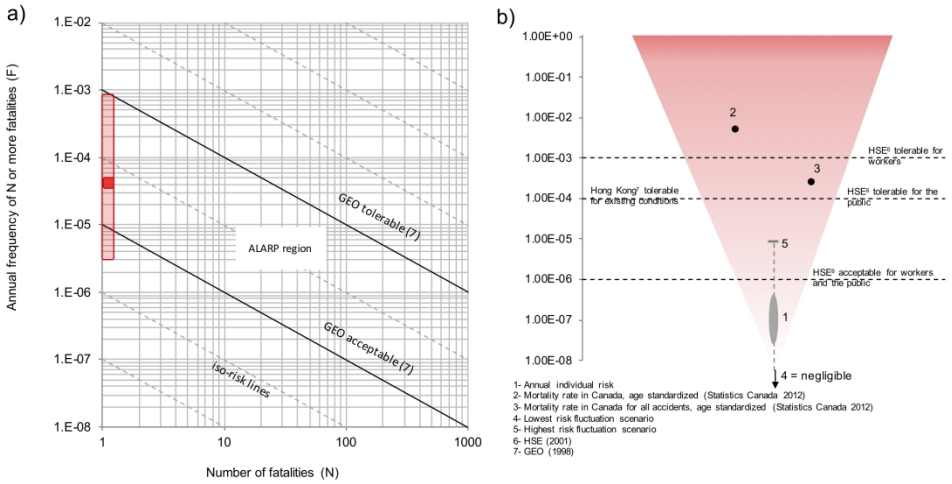

Figure 16 Estimated total (a) and individual (b) residual risk to highway users at the S042 site and plausible ranges. Mortality rates in Canada and criteria proposed for Hong Kong and the HSE in the UK are shown for benchmark

301x150mm (300 x 300 DPI)